Heterogeneous kinetics of the uptake of ClONO2 on NaCl and KBr

ARTICLE *in* THE JOURNAL OF PHYSICAL CHEMISTRY · MAY 1996

Impact Factor: 2.78 · DOI: 10.1021/jp953099i

3 AUTHORS:

Francois Caloz
Diamoond SA
20 PUBLICATIONS **475** CITATIONS
SEE PROFILE

Frederick Frank Fenter
Frontiers Publishing
26 PUBLICATIONS **659** CITATIONS
SEE PROFILE

Michel J Rossi
Paul Scherrer Institut
259 PUBLICATIONS **6,478** CITATIONS
SEE PROFILE

Heterogeneous Kinetics of the Uptake of $ClONO_2$ on NaCl and KBr

François Caloz, Frederick F. Fenter, and Michel J. Rossi*

Laboratoire de Pollution Atmosphérique et Sol (LPAS), Swiss Federal Institute of Technology (EPFL), 1015 Lausanne, Switzerland

Received: October 20, 1995; In Final Form: February 15, 1996[⊗]

The uptake kinetics of $ClONO_2$ on NaCl (reaction 1) and on KBr (reaction 2) have been studied in a low-pressure, Teflon-coated Knudsen reactor at room temperature. The initial uptake coefficient for both reactions has been measured as 0.23 ± 0.06 and 0.35 ± 0.06 for reactions 1 and 2, respectively, and is independent of reactant density in the range $10^{10}-10^{13}$ molecules cm^{-3}. The values of the uptake coefficients are independent of presentation of the salt substrates: identical results are obtained on powder, grains, single-crystal surfaces, and thin deposited salt layers. The only product of reaction 1 is Cl_2. Reaction 2 initially produces Br_2, followed by BrCl and Cl_2. In our proposed mechanism, BrCl is the product of reaction 2, and secondary reactions between BrCl and the KBr substrate yield Br_2 at short reaction times and Cl_2 under prolonged exposure.

Introduction

The heterogeneous reactions of nitrogen oxides with salt are coming under increased scrutiny, with the goal being to understand the role they play in atmospheric chemistry. In particular, nitrogen oxides such as N_2O_5, HNO_3, and $ClONO_2$ have been found to react with salt to produce gaseous chlorine-containing species. If these products are photolyzed in sunlight, then the chlorine atoms thus produced may affect the oxidative potential of the local atmosphere.[1,2] To this end, many efforts are currently underway, including field studies,[3,4] laboratory measurements,[2,5−10] and atmospheric modeling.[11−15] Here, we consider the reactions of gaseous chlorine nitrate with salt, which are characterized by a displacement of halide for nitrate in the condensed phase with a release of the corresponding molecular halogen:

$$ClONO_2 + NaCl \rightarrow Cl_2 + NaNO_3 \quad (1)$$

$$ClONO_2 + KBr \rightarrow BrCl + KNO_3 \quad (2)$$

In the atmosphere, the halogen will photolyze to produce reactive chlorine and bromine atoms. It has been proposed that the chlorine atoms liberated indirectly by the reactions of nitrogen oxides with sea salt aerosol may provide a source of atomic chlorine in the marine troposphere.[16] This source may be competitive with the homogeneous gas-phase reaction between the OH radical and HCl:

$$HCl + OH \rightarrow H_2O + Cl \quad (3)$$

Also, the chlorine and bromine atoms liberated by reactions 1 and 2 may play a role in the catalytic loss of ozone after volcanic injection of salt in the stratosphere, as suggested by *in situ* measurements[17] and modeling.[14]

Keyser and co-workers performed the first quantitative study on reaction 1 at two different temperatures using a flow reactor that significantly deviated from cylindrical symmetry.[5] They found Cl_2 to be the sole product, and they determined the uptake coefficient to be $\gamma = (4.6 \pm 3.0) \times 10^{-3}$ after having applied a correction factor for internal diffusion. These results are in line with the more qualitative conclusions of earlier studies by Finlayson-Pitts and co-workers.[16,18]

Here, we present our kinetic results for reactions 1 and 2, obtained using a low-pressure flow reactor (Knudsen cell). We include a study of the effects of the "internal" surface area of salt samples, presented as powder, grain, single crystals, or spray-deposited films, discussed in the frame of a model proposed by Keyser and co-workers[5,6,19−22] and in light of previous work.[2,9] By systematically varying the presentation of the salt substrate, the reactivity of $ClONO_2$ is studied as a function of surface morphology.

Experimental Section

The experiments are carried out in a low-pressure, Teflon-coated Knudsen reactor described elsewhere.[2] The apparatus consists of a gas-handling system, a Knudsen cell reactor, and a vacuum chamber that houses the mass spectrometer (see Figure 1). Gaseous samples are prepared in the vacuum line and injected into the reactor. From the pressure drop in a calibrated volume, the gas flow (molecules s^{-1}) is directly determined using the ideal gas relation, and the mass-spectrometer signal, for all species of interest, is calibrated against the known flow rate. Flow as small as 5×10^{14} molecules s^{-1} can be directly measured, whereas smaller flow rates are found by extrapolation of the calibration curve. The Knudsen cell is a two-chamber reactor in which the exposure of the reactive substrate is controlled with a plunger (cf. Figure 1). In the absence of reaction, the gas flowing into the cell subsequently leaves via a small orifice into the vacuum chamber. Because the cell is operated in the molecular flow regime, the loss through the aperture is a first-order process with respect to the gas-phase density. We experimentally determine the value of the rate of effusive loss, k_{esc}, for each species and for each aperture size. The parameters for the Knudsen cell are summarized in Table 1. The molecules that effuse out of the Knudsen cell enter the upper volume of a differentially pumped vacuum chamber. The effusive beam is modulated by a tuning fork chopper located at the orifice separating the two chambers and is subsequently sampled by a quadrupole mass spectrometer (Balzers QMA 421). Phase-sensitive detection of the chopped signal using a lock-in amplifier (SRS 830) eliminates background sources. The amplified mass-spectrometer signal is proportional to the flow of molecules exiting the Knudsen cell.

* Author to whom correspondence should be addressed.
[⊗] Abstract published in *Advance ACS Abstracts,* April 1, 1996.

S0022-3654(95)03099-1 CCC: $12.00

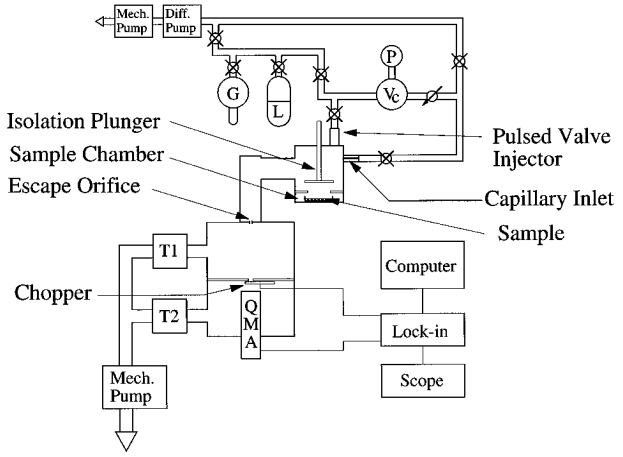

Figure 1. Scheme of the experimental setup. The upper part represents the gas-handling system, including a reservoir for the gaseous reactant (G and L), a calibrated volume (Vc), and a pressure gauge (P) for gas-flow calibrations. The Knudsen cell is mounted on a differentially pumped vacuum chamber, evacuated by two turbomolecular pumps T1 and T2. The flux of gaseous species is measured by a mass spectrometer (QMA) located in the lower of the two vacuum chambers.

TABLE 1: Knudsen Cell Parameters

cell parameter	value
volume	1830 cm^3
estimated surface area (total)	1300 cm^2
surface area (sample)	19.6 cm^2
number density range	$(1-1000) \times 10^{10}$ cm^{-3} [a]
surface collision frequency[b]	67.6 s^{-1}
escape rate constant	
for the 8-mm aperture[c]	$0.80 \times (T/M)^{1/2}$ s^{-1}
for the 9-mm aperture[c]	$1.03 \times (T/M)^{1/2}$ s^{-1}
for the 14-mm aperture[c]	$1.77 \times (T/M)^{1/2}$ s^{-1}

[a] Calculated using the relation $F^i = Vk_{esc}$ [M], where F^i is the flow of molecules, V the reactor volume, and [M] the number density. [b] Calculated for reactive surface of 19.6 cm^2. [c] Determined directly by experiment for $ClONO_2$.

Since the measurement of an uptake rate depends upon the precise knowledge of the escape rate constant (k_{esc}), we determine directly by experiment the true value of k_{esc} for each orifice. The agreement between calculated k_{esc} (from gas-kinetic theory) and the experimentally determined value is found to be in good agreement for diameters under 10 mm; the discrepancy is typically on the order of 20%, i.e., within the uncertainty given by such parameters as reactor volume and true orifice diameter. For larger orifices, the measured value of k_{esc} becomes significantly smaller than that determined from the gas-kinetic expression. We suppose that this effect is due to a perturbation of the molecular velocity distribution.[23] In order to eliminate the uncertainty due to this effect, k_{esc} is measured directly using a series of gases (He, O_2, N_2, SF_6, etc.) for each orifice. The formulas given in Table 1 are valid for all the gases studied.

The experiments described here are based on two distinct experimental procedures, referred to as *steady-state* or *pulsed-valve* experiments. A typical steady-state experiment is carried out by (a) first isolating the surface sample by lowering the plunger and setting a flow of $ClONO_2$ and (b) lifting the plunger to expose the reactive sample to the gas. We measure the first-order rate of uptake, k_{uni}, in terms of the rate of effusive loss from the cell (k_{esc}) and the change in mass-spectrometer signal:[2,24]

$$k_{uni} = k_{esc}\left(\frac{S_i}{S_f} - 1\right)$$

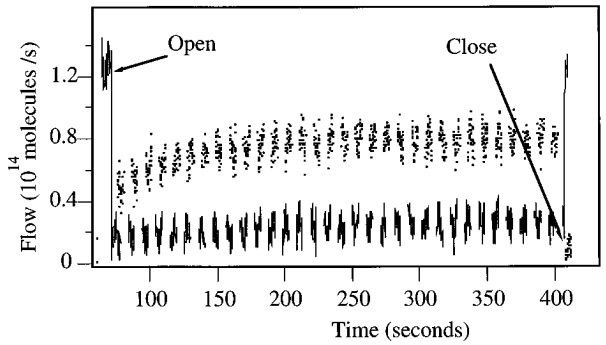

Figure 2. Low-dose steady-state experiments carried out on NaCl powder substrate. The solid line shows the $ClONO_2$ signal at *m/e* 46 (NO_2^+) and the dots give the Cl_2 signal at *m/e* 70 (Cl_2^+). A large decrease in $ClONO_2$ signal is observed when the reactive salt surface is exposed, corresponding to an uptake coefficient of 0.35. Calibration of the signals reveals the Cl_2 yield to be 85 ± 20%.

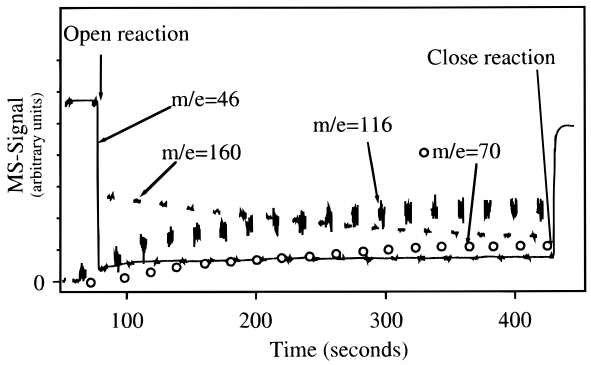

Figure 3. Large-dose, steady-state experiment with KBr powder. $ClONO_2$ flow rate is monitored at *m/e* 46, Br_2 at *m/e* 160, BrCl at *m/e* 116, and Cl_2 at *m/e* 70.

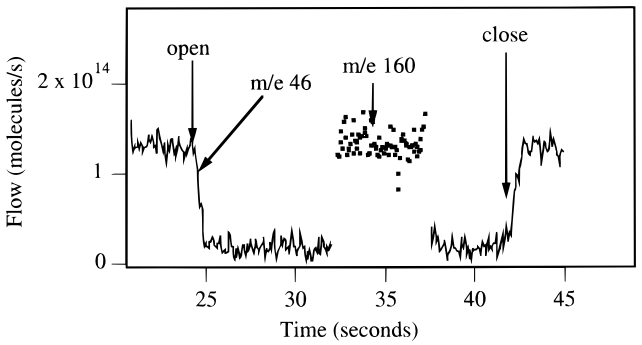

Figure 4. Low-dose, steady-state experiment with KBr powder. The solid line shows the $ClONO_2$ signal at *m/e* 46 (NO_2^+), and the dots give the Br_2 signal at *m/e* 160 (Br_2^+). A large decrease in $ClONO_2$ signal is observed when the reactive salt surface is exposed, corresponding to an uptake coefficient of 0.34. Calibration of the signals reveals the Br_2 yield to be 110 ± 25%.

where S_i and S_f correspond to the signals generated by the effusive beam before and during the interaction between the gas and substrate. Typical signals of steady-state experiments can be seen in Figures 2−4.

A pulsed-valve experiment is carried out by using a solenoid valve, through which gaseous reactant is introduced in millisecond pulses. The "control pulse" is produced while the solid sample is still isolated by the plunger. The "reactive pulse" is obtained by repeating the same operation with the plunger lifted. When the heterogeneous reaction is first order with respect to the gas-phase density, the observed rate of decay, k_{eff}, is simply the sum of k_{esc} and k_{uni} and can be determined by exponential fitting of the obtained signals. Additional kinetic information is gained by characterizing the time-dependent "product pulse",

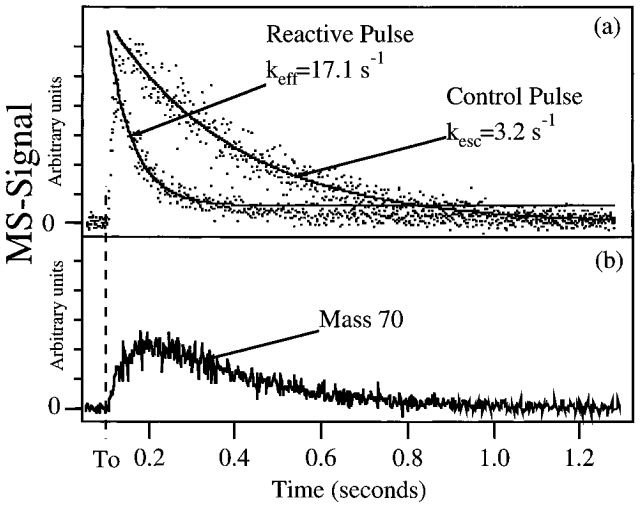

Figure 5. Pulsed-valve experiment performed on powder NaCl sample. This experiment was conducted using the 14-mm orifice. (a) By integration of the "control pulse" (sample isolated), we determine that the pulse contains 4×10^{14} molecules. By exponential fitting of the decay, the effusive rate of loss is measured directly. Exponential fitting of the "reactive pulse" (sample exposed) gives the first-order rate of reactive uptake. In panel b, the simultaneous *m/e* 70 signal (Cl_2^+) is displayed. From the integrations of the "reactive pulse" and the product pulse, we calculate a yield of 110 ± 20% for this experiment.

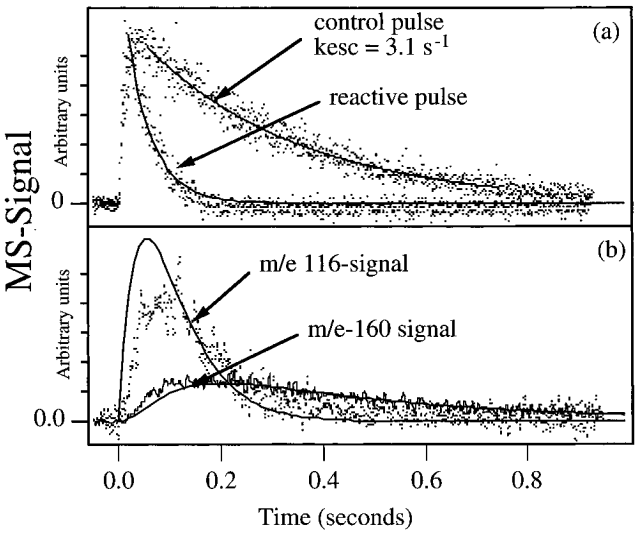

Figure 6. Pulsed-valve experiment on KBr powder. This experiment was conducted using the 14-mm orifice. (a) "Control pulse" and "reactive pulse" obtained as in Figure 5. (b) Simultaneous product pulses of Br_2 at *m/e* 160 and of BrCl at *m/e* 116 (expanded by a factor of 10) are shown. The solid lines through the reactive pulse and through both product traces are obtained by a simple model including only reactions 2 and 4.

obtained by monitoring a product mass peak during the introduction of the reactant. The real-time product profiles thus obtained are useful for understanding (1) the mechanism of the reaction, (2) the extent to which the product itself interacts with the reactive substrate, and (3) the overall mass balance of the reaction. Typical pulsed-valve signals are displayed in Figures 5 and 6. The utility of these experiments is illustrated in the Results section.

The values of γ listed in Tables 2−5 are calculated for experimentally determined k_{uni} using the following expression:

$$\gamma = \frac{k_{uni}}{\omega}$$

where ω is the collision frequency with the reactive surface of 19.6 cm^2 (Table 1) and 15.9 cm^2. The collision frequency is calculated using gas-kinetic theory.[2] In the case of the 14-mm orifice, for which the observed k_{esc} is significantly smaller than the gas-kinetic value, we expect a similar effect for the sample collision rate. The true ω could be smaller than the calculated gas-kinetic value used to calculate the γ's for the experiments performed using the 14-mm orifice; applying a correction would only result in larger values than those reported here.

An important aspect of this work is the use of Teflon and halocarbon wax coatings to render the glass and stainless steel surfaces of the reactor inert. We have two means of testing for an interaction between $ClONO_2$ and the Teflon-coated walls of the reactor. The first is the control experiment in which we leave the sample dish empty and introduce $ClONO_2$ under specific conditions of flow and pressure. When the sample dish is exposed, any reactivity with the Teflon coating becomes evident as a change in the spectrometer signal. This experiment is carried out frequently to verify the quality of the Teflon coating of the sample dish; from these experiments, we determined that the sticking probability of $ClONO_2$ on the coated sample holder is less than 0.01, i.e., much too small to interfere with the kinetic measurements. We can also test for a gas−wall interaction by simply making sure that the value of k_{esc} for $ClONO_2$ scales correctly according to the expressions given in Table 1 for each orifice. This was always the case, indicating that any interaction between $ClONO_2$ and Teflon is unobservable under our experimental conditions.

Preparation of Gaseous Samples. The $ClONO_2$ is synthesized in our laboratory by adding Cl_2O to an excess of N_2O_5, according to the procedure described by Molina and coworkers.[25] The mixture is then stored in a dry ice/methanol bath and subjected to several heating−cooling cycles (between −78 and −25 °C) to accelerate the rate of reaction. The resulting mixture of $ClONO_2$ and N_2O_5 is distilled to yield the final product, a yellow−green liquid that can be stored for several weeks at dry ice temperature. The major impurity of $ClONO_2$ is chlorine, which is eliminated before each experiment with a freeze−pump−thaw cycle. By monitoring the calibrated signal at *m/e* 70 (Cl_2^+), we determine the Cl_2 impurity to be less than 1%. In addition, we detect trace quantities (≪1%) of HNO_3 and HCl in the chlorine nitrate. Liquid Cl_2O is obtained by condensing Cl_2 on an excess of yellow mercuric oxide (HgO) and allowing the mixture to react at a temperature of −78 °C for at least 12 h.[26] Dinitrogen pentoxide (N_2O_5) is synthesized by mixing NO_2 with an excess of ozone, both dried by passage through a P_2O_5 trap, and condensing the product in a dry ice/methanol bath.[9] Gaseous BrCl is obtained by mixing a small amount of Br_2 to an excess of Cl_2 and allowing the mixture to reach equilibrium

$$Br_2 + Cl_2 \leftrightarrow 2BrCl \qquad K^{298} = 7.63^{27}$$

Our working mixtures typically contained 80% Cl_2, 18% BrCl, and 2% Br_2.

Table 6 shows the principal peaks in the mass spectra of the gaseous samples used in the course of this work.

Preparation of Solid Samples. For this study, we used commercial NaCl (Fluka puriss. p.a.) and KBr (Fluka puriss. p.a. ACS). Because of the recent debate concerning the role of diffusion into the interstitial spaces of powder and grain samples, we have studied the reactivity of a range of samples, providing a large variation of the total exposed surface area. Salts are known to be nonporous materials; other laboratories have found that, for example, the BET surface area of salt grain corresponds to the total geometrical surface area.[5] In order to

TABLE 2: (a) Steady-State, (b) Pulsed-Valve, and (c) Yield[a] Experiments on NaCl[b]

salt/type	mass, g	flow, molecules/s	dose, molecules	orifice, mm	k_{esc}, s^{-1}	sample diam, mm	ω, s^{-1}	k_{uni}, s^{-1}	γ	yield
				Section a						
NaCl/powder	1	8.00E+13		9	1.8	50	67.7	16.2	0.24	0.63
NaCl/powder	1	2.50E+14		9	1.8	50	67.7	16.2	0.24	0.81
NaCl/powder	1	8.00E+14		9	1.8	50	67.7	17.1	0.25	1.01
NaCl/powder	1.3	8.50E+14		9	1.8	50	67.7	17.1	0.25	1.05
NaCl/powder	1.2	1.00E+14		8	1.4	50	67.7	12.5	0.18	
NaCl/powder	1	2.20E+14		14	3.0	50	67.7	24.0	0.35	0.64
NaCl/powder	1	1.35E+15		14	3.0	50	67.7	20.2	0.30	0.92
NaCl/powder	1.2	1.00E+14		14	3.0	50	67.7	25.5	0.38	0.72
NaCl/powder	1.2	5.00E+14		14	3.0	50	67.7	11.4	0.17	1.02
NaCl/powder	1.1	1.00E+14		14	3.0	50	67.7	19.8	0.29	1.10
NaCl/powder	1.1	4.90E+14		14	3.0	50	67.7	16.5	0.24	1.02
NaCl/powder	1.2	1.40E+14		14	3.0	50	67.7	21.6	0.32	1.02
NaCl/window		1.00E+15		9	1.8	45	54.9	9.4	0.17	
NaCl/window		5.00E+14		9	1.8	45	54.9	13.3	0.24	
NaCl/window		2.00E+13		9	1.8	45	54.9	11.3	0.21	
NaCl/window		3.00E+13		9	1.8	45	54.9	13.7	0.25	0.40
NaCl/window		1.30E+14		14	3.0	45	54.9	12.9	0.24	0.41
NaCl/grain	1.3	7.00E+14		9	1.8	50	67.7	9.5	0.14	
NaCl/grain	3.2	6.50E+14		9	1.8	50	67.7	9.8	0.15	
NaCl/grain	5.4	7.00E+14		9	1.8	50	67.7	10.8	0.16	
NaCl/grain	12	8.00E+14		9	1.8	50	67.7	10.4	0.15	
NaCl/grain	2.5	6.00E+13		9	1.8	50	67.7	14.4	0.21	
NaCl/grain	2.6	1.50E+14		9	1.8	50	67.7	12.1	0.18	0.69
NaCl/spray	0.004	1.20E+14		14	3.0	50	67.7	17.6	0.26	1.00
NaCl/spray	0.005	1.00E+13		14	3.1	50	67.7	20.3	0.30	
				Section b						
NaCl/powder	1.3		4.00E+14	14	3.2	50	67.7	14.0	0.21	
NaCl/powder	1.5		2.80E+14	14	3.0	50	67.7	18.0	0.27	
NaCl/powder	1.5		3.00E+14	8	1.4	50	67.7	12.6	0.19	
NaCl/powder	1.2		1.50E+14	14	3.0	50	67.7	16.3	0.24	1.00
				Section c						
NaCl/powder	1	1.60E+15		9						0.97
NaCl/powder	1	6.40E+14		9						1.05
NaCl/powder	1	2.80E+15		9						1.04
NaCl/window		4.80E+13		9						0.63
NaCl/powder	1.3	8.00E+14		14						1.08

[a] These experiments are designed to calculate the yield of reaction 1. Surfaces are partially saturated to make sure steady-state conditions are established. [b] The notation E+*n* represents $\times 10^{+n}$ in all tables.

TABLE 3: (a) Steady-State and (b) Pulsed-Valve Experiments on KBr

salt/type	mass, g	flow, molecules/s	dose, molecules	orifice, mm	k_{esc}, s^{-1}	sample diam, mm	ω, s^{-1}	k_{uni}, s^{-1}	γ	yield
KBr/powder	1	9.00E+14		9	1.8	50	67.7	23.4	0.35	0.86
KBr/powder	1	5.70E+14		9	1.8	50	67.7	22.3	0.33	0.9
KBr/powder	1	5.00E+14		9	1.8	50	67.7	23.2	0.34	0.88
KBr/powder	2	5.50E+14		8	1.4	50	67.7	21.1	0.31	1.08
KBr/powder	2	3.60E+14		14	3.0	50	67.7	22.8	0.34	0.9
KBr/powder	2	2.80E+15		14	3.0	50	67.7	20.6	0.30	
KBr/powder	2	4.00E+14		14	3.1	50	67.7	25.0	0.37	
KBr/powder	2	1.00E+14		14	3.0	50	67.7	24.9	0.37	1.14
KBr/window		6.50E+13		9	1.8	50	67.7	21.7	0.32	0.8
KBr/window		1.00E+14		14	3.0	50	67.7	35.7	0.53	0.84
KBr/grain	2	1.90E+15		8	1.4	50	67.7	24.6	0.36	
KBr/spray	0.005	2.00E+13		14	3.1	50	67.7	27.0	0.40	1.1
				Section b						
KBr/powder	1.2		3.80E+14	14	3.1	50	67.7	15.8	0.24	0.8
KBr/spray	0.004		1.10E+14	14	3.0	50	67.7	21.7	0.32	0.7
KBr/powder	1.1		2.00E+14	14	3.1	50	67.7	21.7	0.32	1.05

test the influence of total external surface area on the reactivity of our systems, we carry out experiments on powders, single-crystal optical flats, submillimeter grain samples, and spray-deposited samples. Powders are obtained by grinding salt in a ball mill and then sieving to isolate a size fraction. Typically, we collect powder with grain size between 35 and 100 μm. The total external surface of these samples is large and can be estimated based on electron-microscope images. When the sieving procedure is carried out for salt grain (diameters in the range of 350−500 μm) a monodisperse fraction is obtained with a large and quantifiable total exposed surface area. This is the ideal material for testing the role of diffusion in the internal void of the solid substrates.[9]

TABLE 4: Experimental Results: NaCl + $ClONO_2$

substrate	expt type	no. of expts	uptake γ
powder	steady state	12	0.27 ± 0.07
powder	pulsed valve	4	0.23 ± 0.05
window	steady state	5	0.22 ± 0.04
grain (350 μm)	steady state	6	0.16 ± 0.04
spray deposited	steady state	2	0.28 ± 0.1
			0.23 ± 0.06 av

TABLE 5: Experimental Results: KBr + $ClONO_2$

substrate	expt type	no. of expts	uptake γ
powder	steady state	8	0.33 ± 0.03
powder	pulsed valve	2	0.28 ± 0.1
window	steady state	2	0.42 ± 0.12
grain (350 μm)	steady state	1	0.36 ± 0.1
spray deposited	steady state	1	0.40 ± 0.1
spray deposited	pulsed valve	1	0.32 ± 0.1
			0.35 ± 0.06 av

TABLE 6: Mass-Spectral Data

species	peak 1[a]	peak 2[a]	peak 3[a]	sensitivity[b]
$ClONO_2$	46 (100)	51 (14)	35 (7)	1.255
Cl_2	70 (100)	35 (33)		0.8
Br_2	160 (100)	79 (25)	81 (25)	2.3
BrCl	116 (100)	35 (28)	79 (15)	2.5

[a] Ion mass with peak intensity in parentheses, given as percent of base peak. [b] Sensitivity given in 10^{15} molecules/V, measured at the base peak.

With the single-crystal and spray-deposited samples, we study the reactivity in the absence of the interstitial void present in the grains and powders. Spectroscopy-grade salt windows (Dr. Karl Korth, $\phi = 500$ mm for KBr and $\phi = 45$ mm for NaCl) are typically treated by gliding a sheet of wet optical paper across the surface, followed by rinsing with methanol and drying (corresponding to wet-etched surfaces). The surfaces are alternatively prepared by rubbing with fine-grained sandpaper and subsequent blowing off of the surface powder. Spray-coated optical flats are obtained by vaporizing a saturated salt solution on a heated glass support. Methanol is used as the solvent, and we obtain surface coverage approaching 100%. By depositing only 1−5 mg of salt, the obtained salt film is smooth and nonporous and has a thickness of less than 2 μm. The spray-deposited surfaces are characterized in more detail in previous work.[9]

In general, the samples are pumped overnight after introduction into the Knudsen cell to eliminate residual water.

Results and Discussion

A. $ClONO_2$ + NaCl → $NaNO_3$ + Cl_2. We investigated reaction 1 by a series of steady-state experiments on powder samples. Although most of the experiments are conducted in the limit of small flow rates (to avoid saturation of the uptake), a systematic study of the uptake rate dependence on the $ClONO_2$ flow rate was also carried out. For all the experiments described here, chlorine nitrate is monitored at the *m/e* 46 base peak (NO_2^+). When a chloride sample is exposed to the $ClONO_2$ flow, the rapid loss of signal at *m/e* 46 with new intensity at *m/e* 35, 37, 70, 72, and 74 is observed (cf. Figure 2). From these experiments, we can draw the following conclusions: (a) Cl_2 is the only product of the reaction, and it is formed with a $110 \pm 15\%$ yield, where the estimated error is based on the uncertainties associated with the $ClONO_2$ and Cl_2 flow calibrations. (b) The rate of uptake is independent of the flow of $ClONO_2$, confirming a first-order rate law for the reaction. (c) The uptake coefficient, determined as the average of all the experiments, is $\gamma = 0.27 \pm 0.06$, where the estimated error is the 1σ statistical limit of the mean. As with all our kinetic results described here, we do not include an estimate of systematic error in the reported uncertainties of the rate constants and uptake coefficients due to parameters such as surface roughness; these may represent a source of systematic uncertainty but are difficult to assess for surface reactions that occur with very high sticking probability as measured in this work.

Our conclusions concerning reaction 1 are confirmed by the results of pulsed-valve experiments. In these, *m/e* 46 and 70 signals are calibrated to monitor $ClONO_2$ and Cl_2, respectively, during the milliseconds following the injection of $ClONO_2$ into the reactor. In Figure 5, we show the results of a typical run. The "control pulse" shows the effusive loss of the $ClONO_2$ from the cell when the chloride is still isolated behind the sample plunger. The "reactive pulse" is actuated under exactly the same experimental conditions but with the NaCl sample exposed to the reactor volume. The loss of $ClONO_2$ due to reaction 1 is exponential, and a rate for k_{uni} can be determined directly by a least-squares fitting of the experimental trace. From these experiments, we confirm our earlier conclusion that the uptake is a first-order process with respect to loss of gaseous $ClONO_2$. The value of the uptake coefficient determined from these experiments, $\gamma = 0.23 \pm 0.05$, is in excellent agreement with the value determined by the steady-state experiments. In Figure 5, it can be seen that the Cl_2 signal (*m/e* 70) rises rapidly and then decays according to the rate of effusive loss of chlorine from the reactor. This demonstrates that there is no interaction between the Cl_2 formed as a product and the NaCl substrate.

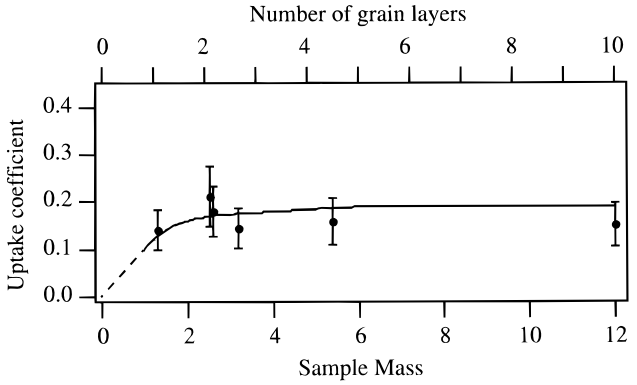

Figure 7. Steady-state experiments performed on NaCl grain. Sieved salt has the average dimension of 350 μm and is held in a 5-cm-diameter dish. Varying the sample mass from 1.2 to 12 g changes the number of grain layers from 1 to 10. The solid curve shows a fit to our data with the model developed by Keyser and co-workers. The $ClONO_2$/NaCl reaction is independent of sample mass over the range of values studied.

In an additional series of experiments, we systematically varied the total exposed surface area of the salt substrates to see if this parameter plays a role in the observed rate of $ClONO_2$ uptake. This dependence is most easily studied in a quantitative manner by varying the number of layers of a monodisperse salt grain within the sample holder. As the mass of the sample increases, so does the interstitial void, and if diffusion into this void is fast, the rate of uptake will increase with the extent to which the sample holder is filled. In Figure 7, we see that there is no variation in the initial rate of uptake of $ClONO_2$ as the sample mass of the monodisperse grain is varied by a factor of 10. In the other extreme of surface presentation, the internal void can be eliminated by studying the reaction with salt single crystals and with spray-deposited surfaces. The results of all the experiments are listed in Table 2 and summarized in Table 4, where it is seen that all of the chloride substrates yield the same uptake probability, within the uncertainties of the experimental measurements. In a later section, we briefly discuss the implications of this finding for the application of correction factors to heterogeneous reaction rate constants on "porous" substrates.

In addition, reaction 1 was studied as a function of gas density by systematically varying the gas-flow and escape orifice for each type of substrate. In Figure 8, we see that the results are independent of the gas density and of the surface presentation, thus confirming the first-order rate law for reactive uptake on reaction 1.

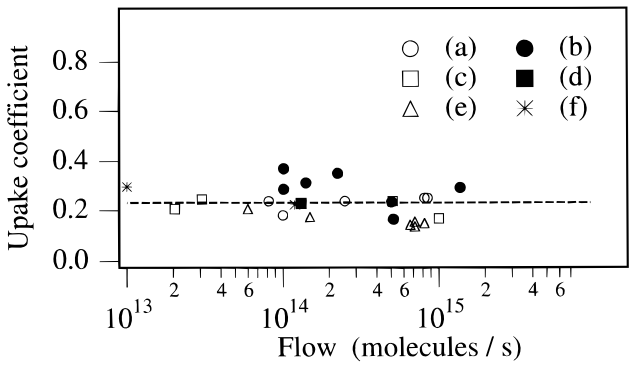

Figure 8. Summary of all the steady-state experiments as a function of flow rate, orifice size, and NaCl sample presentation for reaction 1: (a) powder substrate, 9-mm orifice; (b) powder substrate, 14-mm orifice; (c) window substrate, 9-mm orifice; (d) window substrate, 14-mm orifice; (e) grain substrates, 9-mm orifice; (f) spray-deposited substrates, 14-mm orifice.

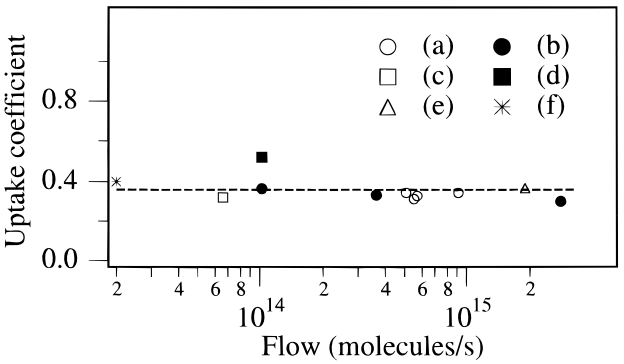

Figure 9. Summary of all the steady-state experiments as a function of flow rate, orifice size, and KBr sample presentation for reaction 2: (a) powder substrate, 9-mm orifice; (b) powder substrate, 14-mm orifice; (c) window substrate, 9-mm orifice; (d) window substrate, 14-mm orifice; (e) grain substrates, 9-mm orifice; (f) spray-deposited substrates, 14-mm orifice.

B. $ClONO_2$ + KBr → products. As with the chloride reaction, we began this study with a series of steady-state experiments on powder substrates. On the basis of our observations of reaction 1, we expected BrCl to be the main or even the sole product of reaction 2. When the bromide powder is exposed to the gas flow, a strong uptake of $ClONO_2$ (*m/e* 46) is observed, but initially, no BrCl is formed (monitored at *m/e* 116, $BrCl^+$). In fact, the only new intensity observed in the product spectrum is found at *m/e* 79 and 81 (Br^+) and *m/e* 158, 160, and 162 (Br_2^+). After prolonged exposure to the reactant, the molecular bromine signal decreases, and BrCl and Cl_2 are produced in small quantities. A typical time-dependent mass scan is displayed in Figure 3 at a flow rate of $ClONO_2$ of 2.8×10^{15} molecules/s. If BrCl is formed as the direct product, it is itself reactive with respect to the bromide to yield Br_2 and with chloride to give Cl_2. As with reaction 1, we carried out most of the experiments at low flow rates of less than 2×10^{14} molecules/s to avoid "saturation" of the substrate (Figure 4). Under these conditions, we find the uptake coefficient to be $\gamma = 0.34 \pm 0.03$, with molecular bromine as the product with $100 \pm 15\%$ yield, where the uncertainty is given by the imprecision of the relevant mass-flow calibrations.

In a series of ancillary steady-state experiments, using authentic samples of BrCl and Cl_2, we confirm that the reactions of BrCl and Cl_2 with bromide are fast:

$$BrCl(g) + KBr(s) \rightarrow Br_2(g) + KCl(s) \quad (4)$$

$$Cl_2(g) + KBr(s) \rightarrow BrCl(g) + KCl(s) \quad (5)$$

Reactions 4 and 5 are characterized by $\gamma > 0.1$ and have unitary yields for the given stoichiometries. In the steady-state experiments described above (Figure 4), the absence of a BrCl signal is not surprising given the rapid conversion to Br_2 in the presence of bromide.

Additional experiments were carried out on spectroscopy-grade bromide windows and on spray-deposited samples. As with the study of reaction 1, the reactivity was also investigated as a function of the $ClONO_2$ flow rate. The results on reaction 2 are listed in Table 3 and summarized in Table 5; in Figure 9, it can be seen that the rate of uptake remains independent of these variables over the range of experimental conditions studied.

We were able to gain additional insight into the kinetics of reaction 2 by following the real-time evolution of the reaction after the pulsed-valve injection of $ClONO_2$ into the reactor. Typical experimental traces are shown in Figure 6, in which $ClONO_2$ (*m/e* 46), BrCl (*m/e* 116), and Br_2 (*m/e* 160) are monitored in real time (in sequential experiments). The decay of the $ClONO_2$ signal corresponds to an uptake probability of 0.30 ± 0.1, in agreement with the value we determined using the steady-state technique. In these experiments, a short-lived BrCl signal is observed. The first-order rate constant for the observed experimental decay of BrCl ($10-15\ s^{-1}$) is much greater than the rate of effusive loss from the reactor ($k_{esc} = 2.9\ s^{-1}$). The Br_2 signal decay, in contrast, is well described by the first-order effusion rate. These observations indicate that the BrCl reacts with the substrate to form Br_2 and that Br_2 does not interact with the bromide. Indeed, a kinetic simulation using only reactions 2 and 4 is capable of reproducing the experimental observations, as shown in Figure 6. The model gives the best agreement with the experimental data if the BrCl yield for reaction 2 is set to 1.0 ± 0.2.

All our observations are consistent with the mechanism in which the $ClONO_2$ reacts with bromide to produce BrCl in 100% yield, with a second reaction between BrCl and bromide responsible for the Br_2 formation. When enough chloride has accumulated on the surface of the salt substrate, it reacts directly with gaseous $ClONO_2$ to form the small amount of Cl_2 observed at long reaction times:

$$ClONO_2(g) + KBr(s) \rightarrow BrCl(g) + KNO_3(s) \quad (2)$$

$$BrCl(g) + KBr(s) \rightarrow Br_2(g) + KCl(s) \quad (4)$$

$$ClONO_2(g) + KCl(s) \rightarrow Cl_2(g) + KNO_3(s) \quad (6)$$

$$Cl_2(g) + KBr(s) \rightarrow BrCl(g) + KCl(s) \quad (5)$$

In Figure 3, the formation of BrCl and Cl_2 at long exposure times is easily interpreted in terms of the mechanism detailed above.

C. Surface Morphology Dependence. With solid substrates, and in particular with powders and grains, it is necessary to consider the extent to which the total exposed surface area and morphology has an influence on the observed rate of uptake of a gaseous species. Recently, Keyser and co-workers[20] have proposed a model, developed originally by Wheeler and others,[28,29] in which the overall rate of uptake can be separated into diffusional and reactive components. Based on the properties of the substrate and assuming Knudsen diffusion into the interstitial void of the grain or powder, correction factors are calculated and applied to experimentally determined values of the uptake coefficient to obtain the reaction probability. This

approach is strengthened by the direct experimental characterization of the appropriate substrate, for example, by scanning electron microscopy.

The need to apply these correction factors is not universally accepted. Hanson and Ravishankara, for example, have shown that the rate of uptake of N_2O_5 and $ClONO_2$ on ice is independent or only weakly dependent of the thickness of the ice coating applied to the walls of their flow-tube reactor under their experimental conditions.[30,31] As pointed out by Keyser et al., the reactions that they chose to study are too rapid to offer a sensitive test of the applicability of the theory.[22] From our previous observations, we put forward the hypothesis that certain "sticky" molecules, such as HNO_3, do not diffuse into the interstitial void of a bulk sample at the gas-kinetic Knudsen rate, so the diffusional contribution to the overall reactivity is smaller than that predicted by the theory proposed by Keyser et al. For other species, notably N_2O_5, the agreement between the predictions of the theory and the experimental observations is remarkably good.

For the two reactions studied here, the correction factors calculated by the theory are small because the reaction probability is large enough so that diffusion represents only a minor perturbation to the rate of overall uptake. For this case, the correction applied would be a function of the total surface exposed due to roughness or particle size. For example, for a surface covered by half-spheres, the correction factor would be about a factor of 2, approximately corresponding to the statistical variability of the uptake coefficient measured (Figures 8 and 9). The curve drawn in Figure 7 shows the prediction of the theory as a function of sample mass for grain samples of average size of 350 μm. Because the uptake probability is so large, no variation in the overall uptake is expected over the range of experimental conditions studied. This reaction therefore does not provide a sensitive test of the theory proposed by Keyser and co-workers. Within the uncertainty of the measurements, all the experiments on all substrates yield the same rate constant for the uptake; this is somewhat surprising given the large variation of surfaces employed and may indicate that $ClONO_2$ is a species that, like HNO_3, should be categorized as sticky. On the basis of these observations and on our previous experience with the reactions of HNO_3 and N_2O_5 with salt, we prefer to report our experimental values without applying the corresponding correction factor.

D. Comparison with Previous Work. The first study of reactions 1 and 2, by Finlayson-Pitts and co-workers,[16,18] provided only qualitative details of the reaction kinetics. Their observations, including the shift in the product spectrum at long reaction times, are in accord with our own.

The only previous *quantitative* study, by Timonen et al.,[5] reports measurements of the uptake probability at two temperatures. The experiment was conducted using a flow tube coupled to a quadrupole mass spectrometer. Although the product analysis is in good accord with ours, their experimentally-determined rates are a factor of 7−8 smaller than those we observed. After correcting their data for the effects of diffusion into the interstitial spaces of their granular sample, they conclude that the true reactive uptake coefficient is about 50 times smaller than the value we report here for the same reaction. The reason for this discrepancy is not evident; one contributing factor may be that they neglected radial gas-phase diffusion in their data analysis. According to the authors calculations, the maximum effect due to radial diffusion is on the order of 10% for their experimental conditions; it has, however, been pointed out by others[32] that the effect is difficult to assess for noncylindrical flow reactors and may in fact be much greater. For a fast reaction, this would have the effect of lowering the observed decay rate relative to its true value.

TABLE 7: Comparison with Similar Reactions

species	γ_{NaCl}[a]	J_{NaCl},[b] s^{-1}	strat. density,[c] molecules cm^{-3}
NO_2	$<10^{-7}$	$<1.4 \times 10^{-10}$	2×10^9
N_2O_5	$(5 \pm 2) \times 10^{-4}$	2.3×10^{-5}	5×10^8
HNO_3	$(2.8 \pm 0.3) \times 10^{-2}$	3.7×10^{-4}	2×10^9
$ClONO_2$	0.24 ± 0.06	1.7×10^{-3}	7×10^8

[a] Values for NO_2 taken from unpublished results. Alternatives values for N_2O_5 ($<1 \times 10^{-4}$), $ClONO_2$ ($(4.6 \pm 3.0) \times 10^{-3}$), and HNO_3 ($(1.3 \pm 0.4) \times 10^{-2}$) can be found in ref 6. [b] Taken from the estimation of ref 13 for post El-Chichon stratospheric salt injection. [c] Densities at 28 km taken from ref 31.

E. Atmospheric Importance. Chlorine nitrate has been predicted to be present in the marine troposphere in pptv concentrations,[11] where it can react with salt-containing marine aerosols according to reactions 1 and 2. Furthermore, $ClONO_2$ is known to be present in the stratosphere, where it can come into contact with salt aerosol after volcanic eruptions.[17] The reactions studied here are potentially of consequence to atmospheric chemistry because of the photolyzable molecular halides produced in reactions 1 and 2. Chlorine atoms are known to play a role in the chemistry of the troposphere, where they initiate hydrocarbon oxidation with great efficiency. The role played by stratospheric chlorine atoms in ozone destruction has been well elucidated.

The impact of reactions 1 and 2 should be considered within a set of possible atmospheric reactions involving salts and nitrogen oxides. Taking the example of the NaCl reactions,

$$ClONO_2(g) + NaCl(s) \rightarrow Cl_2(g) + NaNO_3(s) \quad (1)$$

$$2NO_2(g) + NaCl(s) \rightarrow ClNO(g) + NaNO_3(s) \quad (7)$$

$$N_2O_5(g) + NaCl(s) \rightarrow ClNO_2(g) + NaNO_3(s) \quad (8)$$

$$HNO_3(g) + NaCl(s) \rightarrow HCl(g) + NaNO_3(s) \quad (9)$$

All these reactions have in common the loss of a nitrogen oxide from the gas phase and the release of a volatile chlorine-containing compound. Reactions 1, 7, and 8 produce photolyzable molecules which will directly release chlorine atoms in the atmosphere and will participate in important atmospheric oxidation cycles.

To illustrate the potential role of reaction 1 in the atmosphere, in Table 7 we list some nitrogen oxides, the values of the corresponding uptake coefficients with NaCl, and some typical atmospheric concentrations. In addition, we include estimates for the "rate of loss" of each species after volcanic injection of salt into the stratosphere; these values are obtained according to the approximation described in Michelangeli et al.[13] The rate of loss of $ClONO_2$ in the presence of volcanic salt is seen to be competitive with the rate of loss by photolysis calculated by Michelangeli et al. ($J_{phot} = 1.8 \times 10^{-4}\ s^{-1}$). In the table, it is clear that the very rapid reaction between $ClONO_2$ and NaCl might play an important role in the atmosphere wherever particulate salt comes into contact with $ClONO_2$. The nature of this influence can only be properly assessed by a complete atmospheric model.[33]

Because the uptake experiments were carried out at low water-vapor concentration and at room temperature, the results must be considered as an indication of the relative atmospheric importance of reactions 1, 7, 8, and 9. Since salt is known not to interact with water vapor until the relative humidity has

approached or exceeded the deliquescence point, the relative reactivities presented in Table 7 are valid for the stratosphere and for the dry troposphere.

Conclusions

Our major conclusions can be summarized in the following points: (1) $ClONO_2$ is taken up with very large probability by both chlorides and bromides The values for γ that we determine are roughly a factor of 50 greater than those reported in the only previous quantitative study of the reactions. The sole product of the reaction with chloride is molecular chlorine, obtained in 100% yield. Although, under certain experimental conditions, the apparent product of the $ClONO_2$ reaction with bromide is Br_2, pulsed-valve experiments reveal that BrCl is formed as the primary product and that BrCl is itself extremely reactive with respect to bromide. (2) There is no observable effect of the surface presentation on the overall uptake kinetics. Because of this, we do not apply the correction factor suggested by the treatment proposed by Keyser and co-workers. (3) The very efficient uptake of $ClONO_2$ by chlorides and bromides should be taken into account in chemical modeling of the atmosphere wherever particulate salt is present.

Acknowledgment. Funding for this work was provided by the Office Fédéral de l'Education et de la Science (OFES) as part of the HALIPP subproject of the EUROTRAC program and by the Fonds National de la Recherche Scientifique (FNRS) under Grant 20-37599.93. We thank Professor Hubert van den Bergh for his lively interest and input.

References and Notes

(1) Finlayson-Pitts, B. J.; Pitts, J. N. *Atmospheric Chemistry*; John Wiley & Sons: New York, 1986.
(2) Fenter, F. F.; Caloz, F.; Rossi, M. J. *J. Phys. Chem.* **1994**, *98*, 9801.
(3) Harrison, R. M.; Msibi, M. I.; Kitto, A. M. N.; Yamulki, S. *Atmos. Environ.* **1994**, *28*, 1593.
(4) Platt, U.; Hausmann, M. *Res. Chem. Intermed.* **1994**, *20*, 557.
(5) Timonen, R. S.; Chu, L. T.; Leu, M. T.; Keyser, L. F. *J. Phys. Chem.* **1994**, *98*, 9509.
(6) Leu, M.-T.; Timonen, R. S.; Keyser, L. F. Yung, Y. L. *J. Phys. Chem.* **1995**, *99*, 13203.
(7) Behnke, W.; Krüger, H.-U.; Scheer, V.; Zetzsch, C. *Proc. CEC/EUROTRAC* **1991**, 1.
(8) Behnke, W.; Zetzsch, C. *J. Aerosol Sci.* **1990**, *21*, s229.
(9) Fenter, F. F.; Caloz, F.; Rossi, M. J. *J. Phys. Chem.* **1996**, *100*, 1008.
(10) Behnke, W.; Krüger, H.-U.; Scheer, V.; Zetzsch, C. *Proceedings of EUROTRAC Symposium, 1992*; SPB Academic: The Hague, The Netherlands, 1992; p 565.
(11) Singh, H. B.; Kasting, J. F. *J. Atmos. Chem.* **1988**, *7*, 261.
(12) Parrish, D. D.; Hahn, C. J.; Williams, E. J.; Norton, R. B.; Fehsenfeld, F. C.; Singh, H. B.; Shetter, J. D.; Gandrud, B. W.; Ridley, B. A. *J. Geophys. Res.* **1993**, *98*, 14995.
(13) Michelangeli, D. V.; Allen, M.; Yung, Y. L. *Geoph. Res. Lett.* **1991**, *18*, 673.
(14) Michelangeli, D. V.; Allen, M.; Yung, Y. L. *Geophys. Res.* **1989**, *94*, 18429.
(15) Parrish, D. D.; Buhr, M. P. *Adv. Chem. Ser.* **1993**, 243.
(16) Finlayson-Pitts, B. J.; Ezell, M. J.; Pitts, J. N., Jr. *Nature* **1989**, *337*, 241.
(17) Woods, D. C.; Chuan, R. L.; Rose, W. I. *Science* **1985**, *230*, 170.
(18) Berko, H. N.; McCaslin, P. C.; Finlayson-Pitts, B. J. *J. Phys. Chem.* **1991**, *95*, 6951.
(19) Chu, L. T.; Leu, M. T.; Keyser, L. F. *J. Phys. Chem.* **1993**, *97*, 12798.
(20) Keyser, L. F.; Leu, M. T. *J. Coll. Int. Sci.* **1993**, *155*, 137.
(21) Chu, L. T.; Leu, M. T.; Keyser, L. F. *J. Phys. Chem.* **1993**, *97*, 7779.
(22) Keyser, L. F.; Leu, M. T.; Moore, S. B. *J. Phys. Chem.* **1993**, *97*, 2800.
(23) Motz, H.; Wise, H. J. *J. Chem. Phys.* **1960**, *32*, 1893.
(24) Tabor, K.; Gutzwiller, L.; Rossi, M. J. *J. Phys. Chem.* **1994**, *98*, 6172.
(25) Molina, J. A.; Spencer, J. E.; Johnson, S. N. *J. Chem. Phys. Lett.* **1977**, *45*, 158.
(26) Schack, C. J.; Lindahl, C. B. *Inorg. Nucl. Chem. Lett.* **1967**, *3*, 387.
(27) Stull, D. R.; Prophet, C. B. *JANAF Thermochemical Tables, Publication NSRDS-NBS 37*, 2nd ed.; National Bureau of Standards: Washington, DC, 1971.
(28) Wheeler, A. *Adv. Catal.* **1951**, *3*, 249.
(29) Aris, R. *The Mathematical Theory of Diffusion and Reaction in Permeable Catalysts*; Clarendon: Oxford, 1975; Vol. I.
(30) Hanson, D. R.; Ravishankara, A. R. *J. Phys. Chem.* **1992**, *96*, 2682.
(31) Hanson, D. R.; Ravishankara, A. R. *J. Phys. Chem.* **1993**, *97*, 2802.
(32) Hanson, D. R.; Ravishankara, A. R. *J. Phys. Chem.* **1993**, *97*, 12309.
(33) DeMore, W. B.; Sander, S. P.; Golden, D. M.; Hampson, R. F.; Kurylo, M. J.; Howard, C. J.; Ravishankara, A. R.; Kolb, C. E.; Molina, M. J. *Chemical Kinetics and Photochemical Data for Use in Stratospheric Modeling, Evaluation Number 11*; JPL Publication 94-26; NASA: Washington, DC, 1994.

JP953099I